Ultrasound in Med. & Biol., Vol. 26, No. 8, pp. 1357–1362, 2000

0301-5629/00/$–see front matter

PII: S0301-5629(00)00311-2

● *Clinical Note*

# *IN VITRO* SPATIAL COMPOUND SCANNING FOR IMPROVED VISUALIZATION OF ATHEROSCLEROSIS

S. K. JESPERSEN,* J. E. WILHJELM† and H. SILLESEN‡

Center for Arteriosclerosis Detection with Ultrasound (CADUS), *1B-K Medical A/S, Gentofte, Denmark; †Department of Information Technology, Technical University of Denmark, Lyngby, Denmark; and ‡Department of Vascular Surgery, Gentofte Hospital, Hellerup, Denmark

(*Received* 26 *May* 2000; *in final form* 15 *August* 2000)

**Abstract—A new off-line multiangle ultrasound (US) compound scanner has been built with the purpose of investigating possible improvements in visualization of vascular structure. Images of two formalin-fixed human atherosclerotic plaques removed by carotid endarterectomy were recorded from seven insonification angles over a range of 42° and the individual images were combined (averaged) into a single image (spatial compounding). Compared to conventional B-mode imaging, this multiangle compound imaging (MACI) method features images with reduced angle-dependence, reduced random variation (speckle) and improved delineation of the plaque outline. With the MACI approach, it is, thus, easier to assess *e.g.*, a possible residual lumen of an atherosclerotic artery as well as the level of echogenicity for the different plaque constituents. © 2000 World Federation for Ultrasound in Medicine & Biology.**

*Key Words:* **Ultrasound, Spatial compound imaging, Atherosclerosis, Linear array, *In vitro*, Formalin-fixed plaque.**

## INTRODUCTION

The presence of atherosclerotic lesions (plaque) in the carotid arteries increases the risk of stroke, but surgical removal of the plaque has proven beneficial in reducing this risk (ECST 1998). Unfortunately, ultrasonic assessment of size, shape and type of the carotid atherosclerotic lesions is often seriously limited by poor visualization of the plaque; therefore, clinical determination of degree of stenosis is normally based on measurement of blood velocity estimated by Doppler techniques (Londrey et al. 1991). Recent studies, however, have shown that, in addition to the degree of stenosis, the type of atherosclerotic lesion, (*i.e.*, echo-poor) may be an important pathogenic factor (Elatrozy et al. 1998; Polak et al. 1998). Echolucency appears to be related to amount of lipid in the plaque, whereas stronger reflectivity is related to higher content of fibrous tissue and calcification (Feeley et al. 1991; Grønholdt et al. 1997; Leen et al. 1990). However, the interindividual variation is large and prediction of plaque type in the individual case remains somewhat inconsistent.

There are several reasons for the suboptimal image quality: 1. as mentioned, some plaque materials are anechoic in nature (Picano et al. 1985) and will always be difficult to visualize with ultrasound; 2. other materials of anisotropic nature, such as fibrous tissues, produce echo signals with a strong angle-dependence (Picano et al. 1985), resulting in fluctuations in echogenicity when the transducer is moved and/or rotated; 3. because the pathologic thickening of the carotid wall is seldom larger than 4 mm, the extent of the region of interest on the US image is only approximately 20 wavelengths along the acoustic axis (assuming a transducer frequency of 7.5 MHz and a sound speed of 1540 m/s). Due to the speckle noise in this small US image region, a possible residual lumen, plaque outline and plaque type can often be difficult to determine.

An improved image quality may be obtained by using spatial compound imaging, which can reduce the angle-dependence and speckle noise (Jespersen et al. 1998; O'Donnell and Silverstein 1988; Shattuck and Ramm 1982; Trahey et al. 1986; Wagner et al. 1988). Even though a few spatial compound imaging systems have been constructed in the early 1980s (Berson et al. 1981; Carpenter et al. 1980; Shattuck and Ramm 1982), subsequent publications mainly consider such systems theoretically (Anderson et al. 1997; O'Donnell and Silverstein 1988; Shankar and Newhouse 1985), except for

Address correspondence to: Dr. J. E. Wilhjelm, Technical University of Denmark, Department of Information Technology, Bldg. 344, DK-2800 Lyngby, Denmark. E-mail: wilhjelm@it.dtu.dk

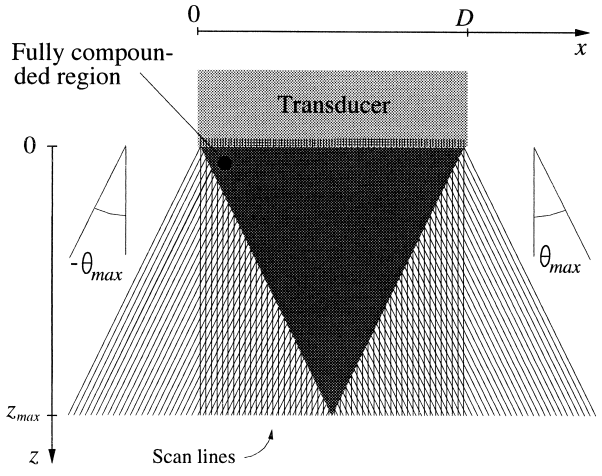


Fig. 1. Conceptual illustration of transducer and associated scan lines for recording of three single-angle images.

the work by Hernandez et al. (1996). In the present work, a digital off-line US scanner for multiangle compound imaging (MACI) was build with the purpose of improving visualization of vascular structures. (Jespersen et al. 1998). Concurrent with our work, the company ATL (Bothell, WA) worked with a similar system operating in real-time that was introduced in the fall of 1999 (Entrekin et al. 1999).

The purpose of the present study was to evaluate if spatial compounding improved the ability of US imaging to visualize formalin-fixed human carotid atherosclerotic plaque, removed during carotid endarterectomy.

## MATERIALS AND METHODS

The MACI system utilizes a conventional low-pitch linear-array transducer. The active aperture is selected as a subset of the elements and this aperture is then operated in phased-array mode, to create a beam with a given angle, $\theta_i$. The aperture is then moved along the entire array to record an image at that angle. This operation is repeated for all desired beam angles, $\theta_i$, where $i = 1, 2, ..., N_\theta$. The final compound image is created by averaging the recorded single-angle images. Figure 1 illustrates the scan lines used in this procedure for $N_\theta = 3$. It is seen that the fully compounded region is a triangle.

The system hardware consists of three major components: 1. A 192-element linear transducer array with center frequency 7.5 MHz, pitch 208 $\mu$m, and transverse acoustical focal distance of 16 mm (Vermont SA, Tours, France). The array length is $D = 40$ mm. 2. A control computer containing a PCI-based 12-bit AD-card and a timing controller (real-time scan controller, RTSC) for the ultrasound system. 3. A 19“ rack containing the custom-designed transmit and receive system hardware, power supply and transducer connector.

The real-time transmit system contains 64 parallel transmitters with fully programmable transmit delays (0 to 34 $\mu$s) and apodization control ($-25$ to - 0 dB). The delay resolution of the transmit system is 16.7 ns. The receive system consists of 64 parallel preamplifiers and a multiplexer that selects one of the receive channels (thus one single-element signal is recorded at a time). This one signal subsequently passes a time gain compensation (TGC) amplifier and an antialiasing lowpass filter before it is digitized in the 12-bit AD converter located in the control computer. The signals can be digitized with a sampling frequency up to 60 MHz.

The system software consists of three main parts: 1. Creation of setup data for the system, 2. Control of the hardware and the recording of the single element signals and 3. processing of the received signals. The digital signal processing performed on the received signals consist of dynamic beamforming, bandpass filtering, envelope detection, scan conversion, compounding, logarithmization, scaling and display. Details can be found in Jespersen et al. (1998).

The size of the point spread function (psf) was measured with a custom-made point scatterer phantom consisting of a single $\approx$100 $\mu$m diameter glass sphere molded into the center of an agar block. The glass sphere was located $\sim$35 mm from the transducer. Images were recorded from 11 different angles in steps of 5°. The $-6$ dB width of the psf measured from the 0° image was 0.7 mm and 0.21 mm, in the lateral and axial directions, respectively. The same measures for the compound image were 0.77 mm and 0.27 mm, respectively. Thus, the spatial compounding increased the psf by no more than $\approx$30%.

Two formalin-fixed carotid plaques (named A and B) were scanned in 3-D cross-sectionally and longitudinally with conventional imaging (0° image) and MACI (averaged image of $-21°$, $-14°$, $-7°$, 0°, 7°, 14° and 21° images). A total of 102 image sets were recorded, each image set consisted of seven single-angle images of 192 parallel scanlines each. The spacing between adjacent image sets was 0.5 mm, obtained by mechanical translation of the array transducer. The plaques were fixed to a special frame by means of four sutures and submerged in pure demineralized degassed water at $\approx$20°C.

## RESULTS

Typical conventional cross-sectional and MACI cross-sectional images from plaque A and plaque B are shown in Figs. 2 and 3, respectively. The axes are given relative to Fig. 1. The *y*-axis is parallel with the longi-

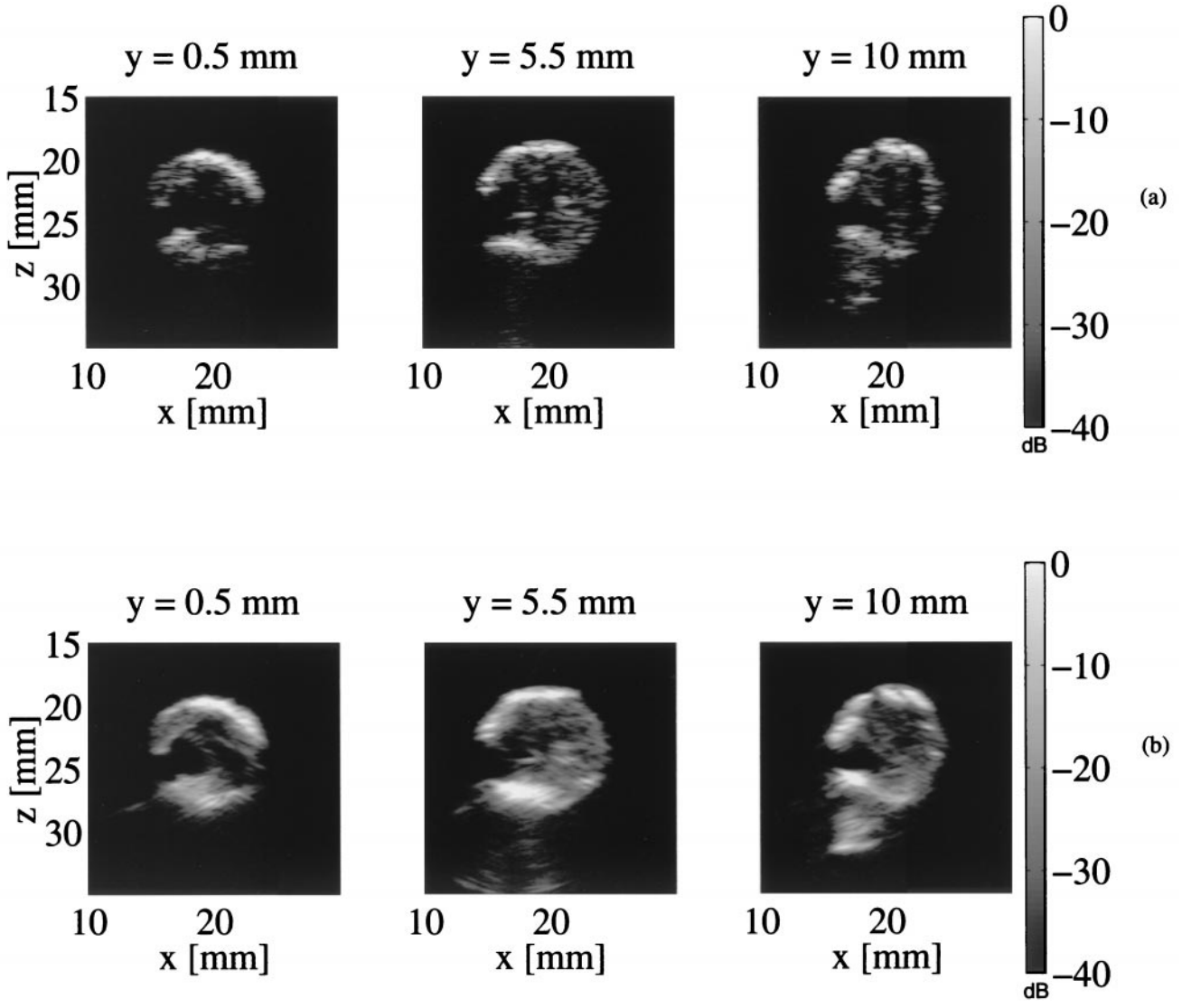


Fig. 2. (a) Conventional and (b) corresponding spatial compound cross-sectional images of formalin-fixed carotid atherosclerotic plaque A.

tudinal axis of the artery. The images in Fig. 2 show plaque from the internal carotid artery. The $y = 1.5$ mm and $y = 4.5$ mm images in Fig. 3 show plaque from the internal carotid artery at the upper part of the image and plaque from the external carotid artery at the lower part. In the same figure, notice, in the images for $y = 1.5$ mm and $y = 4.5$ mm, how the residual lumen is clearly delineated in the spatial compound images compared to the corresponding conventional B-mode image. The y = 11 mm images in Fig. 3 show the smaller amount of plaque in the common carotid artery. Because the plaques were removed by endarterectomy, they are likely to contain the intima layer and some part of the media layer of the artery from which they were removed.

Figure 4 shows the individual single-angles images used to produce the compound image in the first column of Fig. 3. The $\theta_a = 0°$ image corresponds to the conventional B-mode image. Notice the rather poor definition of the outline (and the lumen) in the single-angle images, compared to the corresponding compound image. Note, however, because the plaque specimens were scanned in water (which has low attenuation), the images recorded with the largest beam angles (where the distance between transducer and plaque is the largest), were compensated too much by the TGC. This can be seen in Fig. 4 (the images recorded at large $\theta_i$ are brighter than those recorded at smaller $\theta_i$).

Figure 5 shows an example of a longitudinal scan

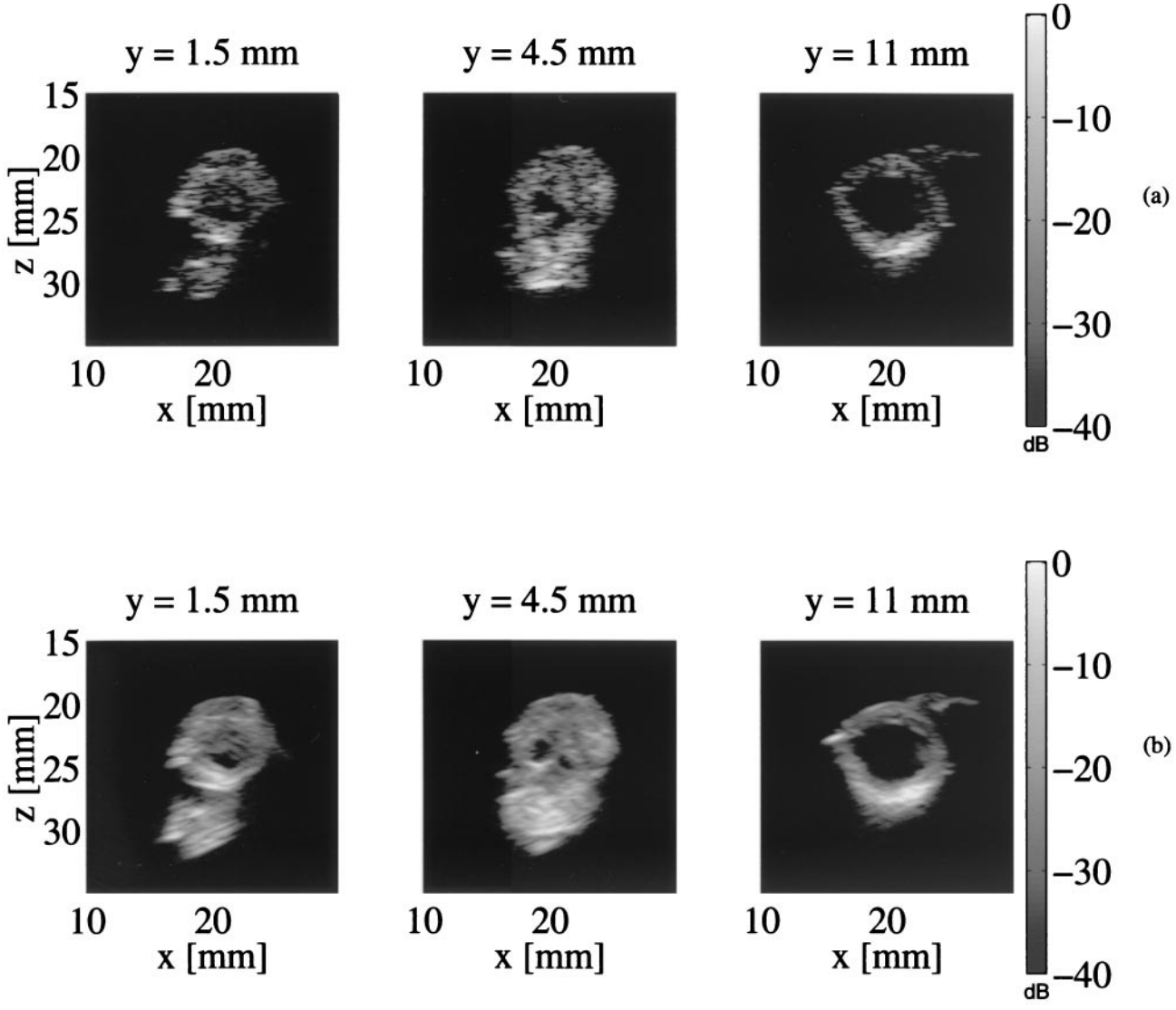


Fig. 3. (a) Conventional and (b) corresponding spatial compound cross-sectional images of formalin-fixed carotid atherosclerotic plaque B.

(scan plane parallel with the longitudinal axis of the transducer) obtained from the plaque A. Notice how the strongly reflecting structure located at $(x, z) = (17$ mm, 26 mm) is creating reverberations beneath it in Fig. 5a. Due to the spatial compounding, this reverberation region has a fan-like shape in Fig. 5b.

## DISCUSSION

When comparing the conventional B-mode images to the multiangle compound images, it is observed that the MACI method features images with reduced angle-dependence, reduced random variation and improved delineation of the plaque outline. These improvements are due to the fact that more scan lines are perpendicular or nearly perpendicular to the tissue interfaces or fibres and also because spatial compounding strongly reduces the variance of the speckle pattern. With the MACI approach, it may be easier to assess, *e.g.*, a possible residual lumen of an atherosclerotic artery, as can be seen by comparing the first and second B-mode images in Fig. 3a with the corresponding images in Fig. 3b.

Another potential advantage of MACI is within quantitative analysis of the images. Because more independent data are recorded from the same tissue region, the speckle is reduced and estimates of parameters such as mean echogenicity should, therefore, be correspondingly more robust, compared with conventional B-mode imaging.

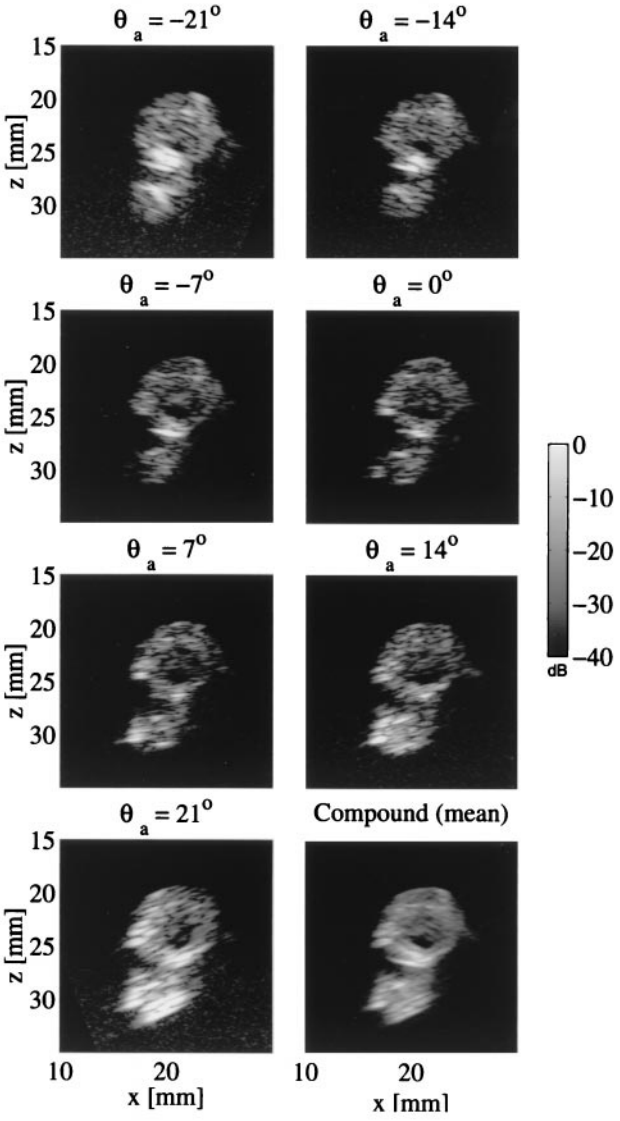


Fig. 4. The seven single-angle images used to create the spatial compound image in Fig.3. This image is repeated in the lower right-hand plot. The $\theta_a = 0°$ image is the conventional B-mode image.

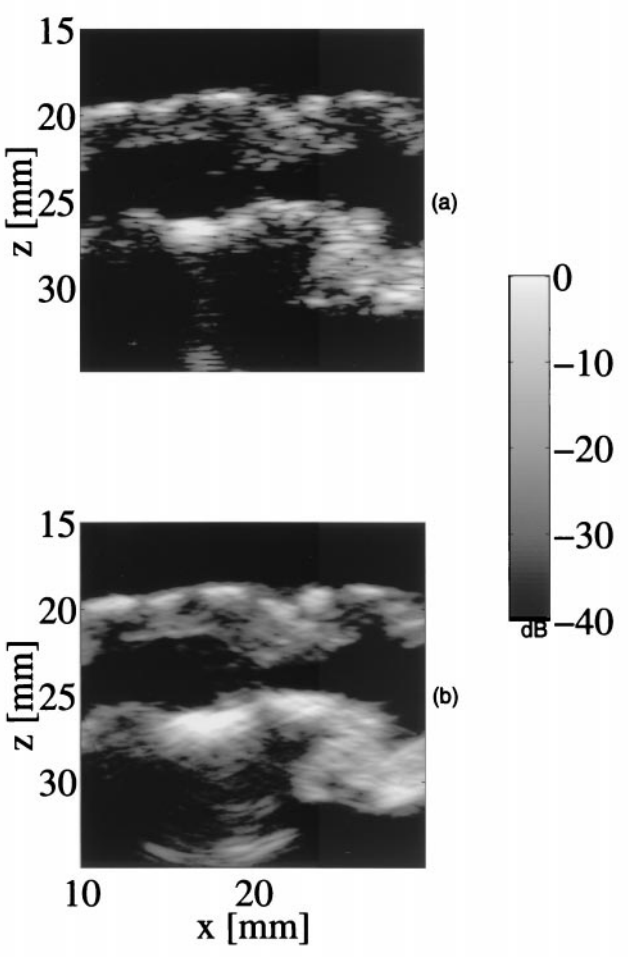


Fig. 5. (a) Conventional and (b) corresponding spatial compound longitudinal images of formalin-fixed carotid atherosclerotic plaque A.

However, considering what appears to be a substantial improvement in imaging capabilities of B-mode US using MACI, one should keep in mind that comparisons to a "golden standard", *i.e.*, histologic analysis, is essential before final conclusions may be drawn.

In spite of the encouraging images obtained in this study, it should be pointed out that a number of factors may influence the achievable image quality *in vivo*. Three of them are based on the fact that single images are recorded and then added (Jespersen et al. 1998):

1. Errors in the assumed mean speed of sound will cause blurring of the resulting compound image, both because the focusing in the individual images will degrade and because the individual single-angle images will be associated with a range and steering angle error causing the images recorded from different directions to be misaligned when added.

2. Tissue movement might also cause image blurring: because the individual single-angle images are recorded consecutively, these might not align exactly when added to form the compound image. This has been studied previously (Jespersen et al. 1998), and an estimate based on typical movement data for the carotid artery gave a maximal displacement that was approximately half of the −6-dB axial width of the psf.

3. Finally, spatial variation in the speed of sound of the tissue being scanned may cause blurring as well, due to local misalignment between the individual single-angle images.

The combined effect of these factors can, however, only be assessed with a system capable of scanning

real-time *in vivo*. The fourth important limitation is technological in nature:

4. When US images are recorded with a beam angle different from zero, grating lobes might occur, depending on how fine a pitch (distance between centers of adjacent transducer elements) is used in the linear-array transducer. Too high grating lobe levels will severely reduce the contrast resolution of the individual single-angle images for high beam angles and thereby also (to a lesser degree) the final compound image. Thus, a consequence can be that the brightness of anechoic (*e.g.*, fatty) regions will be mainly governed by the level of the grating lobes. Because the levels of the grating lobes decrease with pitch, a possible solution is to decrease the pitch. However, if the length of the transducer array is to be kept constant, this can only be done by increasing the number of transducer elements and, thereby, if the size of the transmit/receive aperture is to be kept constant as well, the number of channels in the US system.

## SUMMARY

A new implementation of an imaging modality, Multi-Angle Compound Imaging, has been described and *in vitro* images of carotid plaque specimens showing reduced speckle variation and reduced angle-dependence have been presented. The results appear to reveal a better definition of outlines and a more uniform representation of tissue parameters, compared to conventional B-mode imaging. Therefore, MACI is believed to have potential for improving diagnosis of atherosclerotic disease.

*Acknowledgements*—CADUS is supported by the Danish Technical and Medical Research Councils. The authors gratefully acknowledge the help of Dr. M-L. Moes Grønholdt in providing the specimens and the help by instrument maker K. Martinsen for making the fixtures for the transducer and the biologic specimens.

## REFERENCES

Anderson ME, Soo MS, Bentley RC, Trahey GE. The detection of breast microcalcifications with medical ultrasound. J Acoust Soc Am 1997;101:29–39.

Berson M, Roncin A, Pourcelot L. Compound scanning with an electrically steered beam. Ultrason Imaging 1981;3:303–308.

Carpenter DA, Dadd MJ, Kossoff G. A multimode real time scanner. Ultrasound Med Biol 1980;6:279–284.

Elatrozy T, Nicolaides A, Tegos T, Griffin M. The objective characterisation of ultrasonic carotid plaque features. Eur J Vasc Endovasc Surg 1998;16:223–230.

Entrekin R, Jackson P, Jago JR, Porter BA. Real time spatial compound imaging in breast ultrasound: Technology and early clinical experience. Medicamundi 1999;43:3:35–43.

ECST (European Carotid Surgery Trialist' Collaborative Group). Randomized trial of endarterectomy for recently symptomatic carotid stenosis: Final results of the MRC European Carotid Surgery Trial. Lancet 1998;351:1379–1387.

Feeley TM, Leen EJ, Colgan MP, Moore DJ, Hourihane DO, Shanik GD. Histologic characteristics of carotid artery plaque. J Vasc Surg 1991;13:719–724.

Grønholdt MLM, Wiebe BM, Laursen H, Nielsen T, Schroeder TV, Sillesen H. Lipid-rich carotid artery plaques appear echolucent on ultrasound B-mode imaging and may be associated with intraplaque hemorrhage. Eur J Vasc Endovasc Surg 1997;14:439–445.

Hernandez A, Basset O, Chirossel P, Gimenez G. Spatial compounding in ultrasonic imaging using an articulated scan arm. Ultrasound Med Biol 1996;22:229–238.

Jespersen SK, Wilhjelm JE, Sillesen H. Multi-angle compound imaging. Ultrason Imaging 1998;20:81–102.

Leen EJ, Feeley TM, Colgan MP, O'Malley K, Moore DJ, Hourihane DO, Shanik GD. "Hemorrhagic" carotid plaques does not contain hemorrhage. Eur J Vasc Surg 1990;4:123–128.

Londrey GL, Spadone DP, Hodson KJ, et al. Does color-flow imaging improve the accuracy of duplex carotid evaluation? J Vasc Surg 1991;13:659–662.

O'Donnell M, Silverstein SD. Optimum displacement for compound image generation in medical ultrasound. IEEE Trans UFFC 1988; 35:470–476.

Picano E, Landini L, Distante A, Salvadori M, Lattanzi F, Masini M, L'Abbate A. Angle dependence of ultrasonic backscatter in arterial tissues: A study in vitro. Circulation 1985;72:572–576.

Polak JF, Shemanski L, O'Leary DH, Lefkowitz D, Price TR, Savage PJ, Brant WE, Reid C. Hypoechoic plaque at US of the carotid artery: An independent risk factor for incident stroke in adults aged 65 years or older. Cardiovasc Health Study Radiol 1998;208:649–654.

Shankar PM, Newhouse VL. Speckle reduction with improved resolution in ultrasound images. IEEE Trans Son Ultrason 1985;32:537–543.

Shattuck DP, Ramm OTv. Compound scanning with a phased array. Ultrason Imaging 1982;4:93–107.

Trahey GE, Smith SW, Ramm OTv. Speckle pattern correlation with lateral aperture translation: Experimental results and implications for spatial compounding. IEEE Trans UFFC 1986;33:257–264.

Wagner RF, Insana MF, Smith SW. Fundamental correlation lengths of coherent speckle in medical ultrasonic images. IEEE Trans UFFC 1988;35:34–44.